SAND2013-5968C

Interaction of Defects with Quantum Well States: Electrostatic-Dependant Response Time for Traps in AlGaN/GaN HEMTs

R. J. Kaplar[1], S. DasGupta[1], M. Sun[2], S. Atcitty[1], M. J. Marinella[1], and T. Palacios[2].

[1]Sandia National Laboratories, PO Box 5800, MS 1084, Albuquerque, NM 87185-1084
[2]Massachusetts Institute of Technology, Cambridge, MA 02139.

Recovery transients in high-voltage AlGaN/GaN HEMTs following both blocking voltage and ON-state stress show strong dependence on stress time. The defect time constant spectra exhibit a temperature-dependant component (TG1, E_a = 0.6 eV) and a temperature-independent component (TG2). With increased stress time and larger current collapse, the time constants for TG2 become progressively longer. The stress-time-dependent behavior of TG2 is shown to be consistent with the capture of trapped carriers in the AlGaN barrier directly by quantum well states, originating from the same defect giving rise to the 0.6 eV behavior. By modulating this alternate recombination pathway, the electric field normal to the AlGaN/GaN interface is shown to have a strong effect on reducing the response time of the trap to several orders of magnitude below its bulk response time. This demonstrates that barrier design may be utilized to tune the recovery characteristics of the HEMT.

Introduction

Recently, AlGaN/GaN High Electron Mobility Transistors (HEMTs) have seen widespread application in RF electronics. However, the ease of achieving a low on-state resistance resulting from high channel mobility (μ_{ch}) coupled with high breakdown field due to the wide bandgap of GaN (E_g = 3.4 eV) has led to significant advancements in developing the AlGaN/GaN HEMT as a device for the next generation of high-voltage power electronics [1-4]. Understanding the characteristics of defects in the AlGaN/GaN material system is a key factor in developing power devices with improved performance and reliability. Most techniques for characterizing defects use a bias condition to fill the traps (like the filling pulse in Deep Level Transient Spectroscopy). Following this, optical or thermal excitation is used to study emission of the trapped carriers. However, either in a simple material stack (like a Schottky diode) or in a device such as the HEMT under realistic operation conditions, trapped electrons are assumed to be thermally or optically emitted to the conduction band. Interaction of trapped carriers with the quantum well levels is usually not considered to influence the transient characteristics.

In switching applications, traps that are much slower than the switching time lead to parametric shifts, such as threshold voltage (V_{th}) shift or increase in on-state resistance (R_{ds}) over time. Faster traps with time constants on the order of the switching time lead to distortions in the switching waveform, affecting output power quality [5,6]. Electric field management is generally understood to be important for breakdown voltage enhancement in power devices.

In this study, we demonstrate strong stress-time-dependent behavior for detrapping time constants from deep defect levels near the AlGaN/GaN heterointerface in the HEMT. A temperature-independent detrapping component becomes progressively slower

as the stress time is increased. This behavior is shown to be consistent with the capture of trapped carriers in the AlGaN barrier directly by quantum well states. We show that the presence of the quantum well reduces the response time of the trap by several orders of magnitude below its thermal emission time in the bulk material, and the effect is influenced strongly by the field normal to the AlGaN/GaN interface. The strong influence of electric field on the trap response time indicates that electric field management likley has an important role in the switching performance of the AlGaN/GaN HEMT.

Device Details

The tested devices were fabricated at Massachusetts Institute of Technology on silicon (111) substrates. The devices were designed to achieve a maximum breakdown voltage of 1800V. The devices had gate-to-drain spacing (L_{gd}) ranging from 1.5 to 40 µm, gate-to-source spacing L_{gs} = 1.5 µm, and gate length L_g = 2 µm. These devices used $Al_{0.15}Ga_{0.85}N$ for the 50-nm thick barrier and had a threshold voltage (V_{th}) of ~ −4.1 V. The HEMTs used 4 µm epilayers with a carbon-doped 2.4 µm buffer and 1.4 µm of i-GaN, and the channel GaN was 200 nm thick. The surface passivation was an $Al_2O_3/SiO_2/Al_2O_3$ stack deposited by atomic layer deposition, and was deposited after the gate. A few monolayers (< 2 nm) of gallium oxide, resulting from oxygen plasma treatment before gate pattering, act as the gate dielectric [7]. No field plates were used in the structure.

Bias Time Dependence of Detrapping Transients

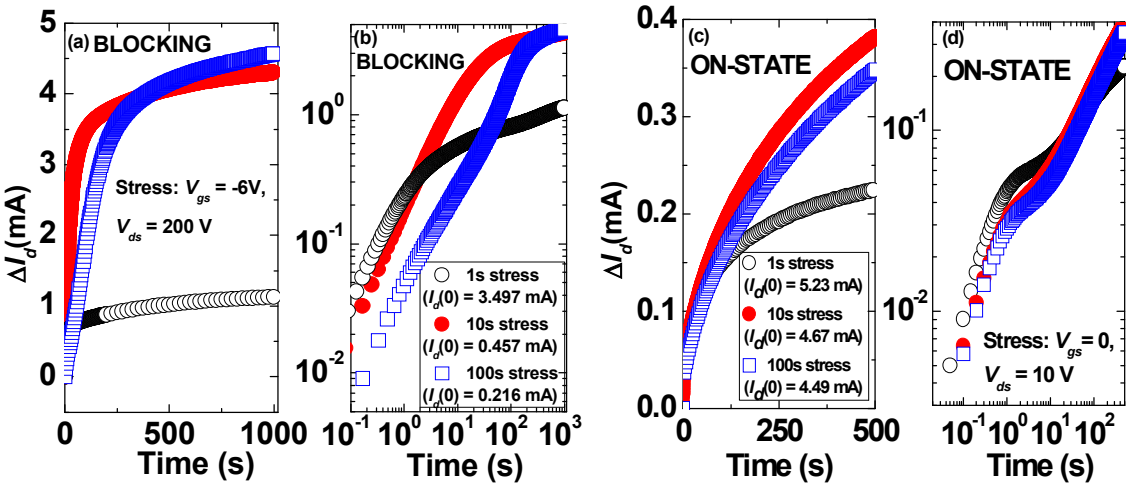

Fig. 1. Detrapping transients (V_{ds} = 1V, V_{gs} = 0) in a passivated $Al_{0.15}Ga_{0.85}N$/GaN HEMT (L_g = 2µm, W_g = 100µm, L_{gd} = 10µm) following blocking voltage stress (V_{gs} = -6 V, V_{ds} = 200 V) for 1s, 10s and 100s on (a) linear and (b) log scales. Pre-stress I_d (V_{ds} = 1 V, V_{gs} = 0) = 4.91 mA. Detrapping transients (V_{ds} = 1V, V_{gs} = 0) following ON-state stress (V_{gs} = 0, V_{ds} = 10 V) for 1s, 10s and 100s on (c) linear and (d) log scales. Pre-stress I_d (V_{ds} = 1 V, V_{gs} = 0) = 5.51 mA.

The devices were stressed in complete darkness with V_{gs} ~ -6 V at V_{ds} = 200 V (blocking voltage state) or V_{ds} = 10 V at V_{gs} = 0 (ON-state). The stress voltage was applied for variable periods of time, following which the detrapping transient was recorded at V_{ds} = 1 V, V_{gs} = 0. Prior to every stress, the drain current (I_d) was completely

recovered to the pre-stress value by shining the probestation microscope light (a halogen lamp) on the sample. Thus, all the effects to be described in subsequent sections are related to variations in occupancy of pre-stress traps. There was no indication of permanent degradation or reduction in I_d at any stage of the experiments. The current transient method (described in [8]) was used to characterize the trapping components.

Fig. 1 shows the detrapping transients following blocking voltage stress (V_{gs} = -6 V, V_{ds} = 200 V) for 1s, 10s and 100s stress times. The recovery transients were measured at V_{gs} = 0, V_{ds} = 1 V. Fig 1a clearly shows that the absolute amount of drain current recovery remains smaller for detrapping following the 100s stress than for detrapping following 10s stress for the first ~100s. Fig. 1b (showing the same data on a log scale) shows that ΔI_d is greater for detrapping following 10s stress than detrapping following 1s stress for the first ~2s.

Figs. 1c and 1d show similar detrapping transients following ON-state voltage stress (V_{gs} = 0, V_{ds} = 10V) for 1s, 10s, and 100s duration. Although less pronounced than in Fig. 1a, the reduced ΔI_d with increased stress time is clearly visible, similar to detrapping following the blocking voltage stress.

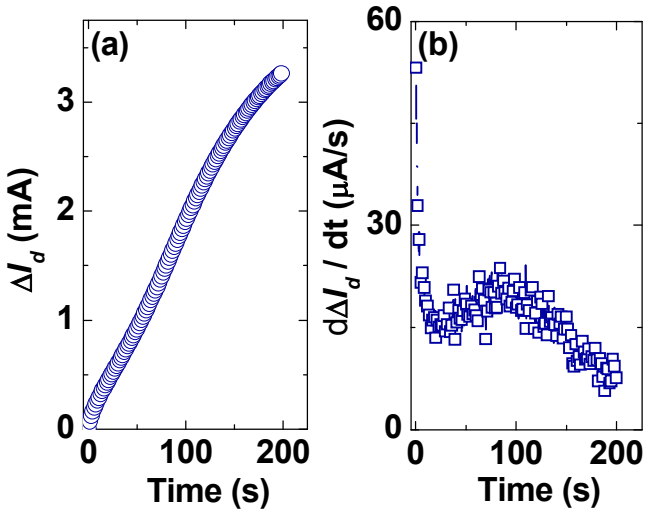

Fig. 2. (a) First 200s of the detrapping transient (V_{ds} = 1V, V_{gs} = 0) shown in Fig. 1 following blocking voltage stress (V_{gs} = -6V, V_{ds} = 200V) for 100s and (b) time derivative of the detrapping transient.

The results in Fig. 1are not possible for a trap or a combination of traps with fixed emission time constants for the following reason. If we compare the transients following 10s and 100s stress, the stress conditions are the same for the first 10s. Therefore, at least the component of trapped charge emitted following the 10s stress should also appear in the transient following the 100s stress. Thus for all times, ΔI_d(t) following 100s stress should be the same or greater, but never smaller than ΔI_d(t) following 10s stress. The fact that Fig. 1 show the exact opposite of this is clear evidence that the trap response time slows down as the stress time is increased.

Also, a careful observation of the first 200s of the detrapping transient following the 100s blocking voltage stress reveals that the transient has an increasing time derivative between ~25 and ~75s (Fig. 2). If we consider the detrapping transient to be composed of a number of exponential detrapping transients with amplitudes A_i and time constants τ_i, then

$$\Delta I_d(t) = \Sigma a_i(1-\exp(-t/\tau_i)), \text{ or } \partial\Delta I_d(t)/\partial t = \Sigma(a_i/\tau_i)\exp(-t/\tau_i) \quad (1)$$

Clearly, for a fixed set of τ_i, the time derivative in eqn. 1 can never increase with time. Thus, Fig. 2 conclusively shows that the trap response times are long at the start of the detrapping process ($t = 0$), and decrease as detrapping proceeds.

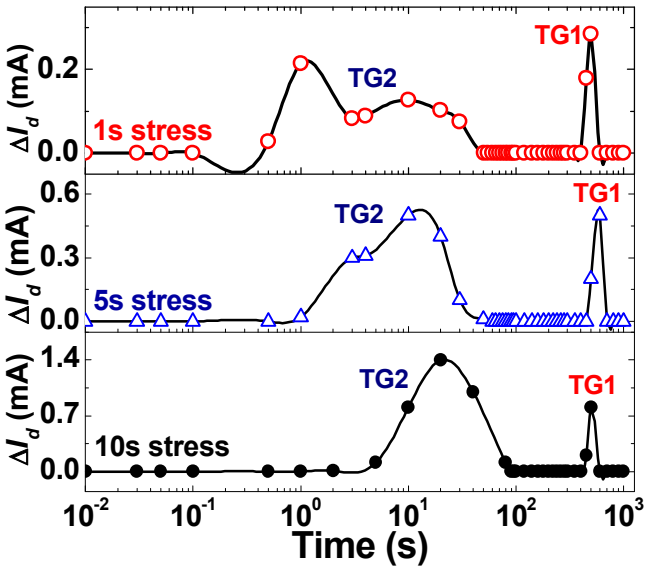

Fig. 3. Extracted time constant spectra from room-temperature detrapping transients for blocking voltage stress (V_{gs} = -6 V, V_{ds} = 200 V) for 1s, 5s, and 10s. Stress time dependence of transients can be seen to come from TG2.

The transients for longer stress times do not fit a sum of decaying exponentials with fixed time constants very well (Fig. 2) for reasons described in the last paragraph, and hence the analysis was done for stress times ranging from 1 to 10 sec. Fig. 3 shows the extracted time constant spectra from detrapping transients after blocking voltage stress (V_{gs} = -6 V, V_{ds} = 200 V) for 1s, 5s and 10s at room temperature. The time constant spectra shows two major components: TG1 at ~500s, and TG2, which is more distributed in time with almost a continuum of time constants spanning over an order of magnitude. The amplitudes of both components increase with increasing stress time. As the stress

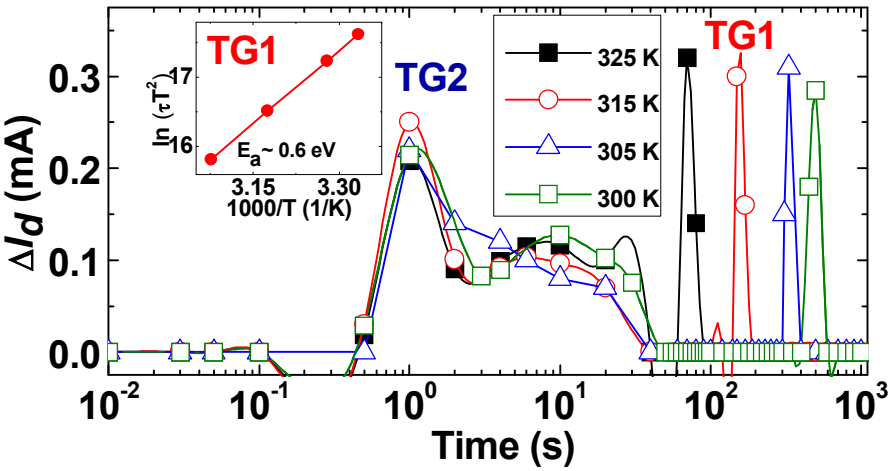

Fig. 4. Extracted time constant spectra from detrapping transients for blocking voltage stress (V_{gs} = -6 V, V_{ds} = 200 V) for 1s at 300K, 305K, 315K and 325K. TG1 shows temperature dependence, but TG2 does not.

time is increased from 1s to 10s, TG2 progressively shifts to higher time constants, but TG1 is invariant in time. Thus, TG2 is the component of trapping which is responsible for the stress time dependence of the detrapping transients.

Fig. 4 shows the temperature dependence of the two trapping components TG1 and TG2. Extracted time constant spectra for detrapping transients following 1s blocking voltage stress are shown over the range 300 to 325K (Fig. 4). TG1 shows a clear temperature dependence with activation energy E_a ~ 0.6 eV, whereas TG2 shows negligible temperature dependence (Fig. 4). The component with E_a ~ 0.6 eV has been observed in multiple studies of charge trapping in the AlGaN/GaN device literature [8-13].

Increase in TG2 time constant: Thermal Emission, Electron Capture and Tunneling

The increase in the detrapping time constant of TG2 with increasing stress time can be due to (a) reduced thermal emission, (b) an increase in electron capture by the defect level during the recovery bias (V_{ds} = 1 V, V_{gs} = 0), or (c) reduced tunneling from the trap level. Hole emission or capture can be ignored in this wide-bandgap majority-carrier device.

(a): Reduced Thermal Emission: At a given temperature, decreased thermal emission rate can be caused by a decrease in the defect capture cross section or a change in the defect energy level to a value further from the conduction band. Such physical changes to the defect or emergence of new defects constitute permanent degradation. It should be remembered that no sign of permanent degradation was observed during any stress experiment. As stated at the beginning of Section III, any current collapse was completely recoverable in less than 1s by shining the probestation microscope lamp on the sample. Thus, the change in the time constant of TG2 is unrelated to creation of new defects, as observed in hot-carrier degradation or the inverse piezoelectric effect [9, 14-16]. Without creation of new defects or physical changes to existing defects, reduced thermal emission can be ruled out as the reason for the increase in the time constant of TG2.

The other factor to consider within the context of reduced thermal emission is the variation of channel temperature with channel current and its influence on the emission time constant of the traps [17-19]. As Fig. 1 shows, the biggest change in detrapping rate with stress time is observed between 10s and 100s for blocking voltage stress, where the post-stress current $I_d(0)$ changes from ~0.45 mA to ~0.22 mA. However, in spite of a much bigger difference in $I_d(0)$ from ~3.5 mA to ~ 0.45 mA, the change in detrapping rate is much smaller between 1s and 10s stress than between 10s and 100s stress. Thus it is unlikely that the decreased detrapping rate with increased bias time is related to variations in channel temperature or channel current. In any case, most of the bias-dependant variation is shown to come from a trapping component with negligible temperature dependence. The temperature-independent nature of TG2 also rules out combined thermal and electrostatic effects like field-enhanced emission, which shows a clear temperature dependence that grows weaker with increasing electric field.

(b): Increase in electron capture during recovery bias (V_{ds} = 1 V, V_{gs} = 0)*:* Enhanced electron trapping due to increased stress time can significantly alter the conduction band profile and hence the electron distribution in the device. If the change in the band profile causes the free electron density to locally *increase* at the location of TG2, there can be an overall slowdown in the detrapping of TG2.

An increase in trapped electron density tends to increase the conduction band energy and *reduce* electron current in a semiconductor. However, in the GaN HEMT, injection of electrons from the gate electrode influences the electron density in the device. An *increase* in the level of gate injection from the altered conduction band profile post-stress could explain enhanced electron capture at TG2 during recovery bias, and hence an increase in time constant for TG2. However I_g *decreases* after both ON-state and blocking voltage stress for all V_{gs} from OFF-state to recovery bias (V_{gs} = 0). This rules out the increase in electron capture during recovery bias as the reason for an increase in detrapping time for TG2.

(c): Reduced Tunneling from the Trap Level: Since both reduced thermal emission and enhanced electron trapping have been shown to be inconsistent with the experimental observations, reduced tunneling from the trap level is the only possible explanation for the stress-time dependant behavior of TG2.

To understand the dependence of detrapping time constants on stress time, we perform self-consistent 1D solutions of the Schrödinger and Poisson equations on the HEMT structure for different trapping magnitudes. The two cases shown in Fig. 5a are (a) Electron trapping in the AlGaN with a density of 10^{17}cm^{-3}, ranging in spatial extent from the AlGaN/GaN interface to a distance 7.5 nm from the interface, emulating the trapping for shorter stress time, such as 10s; and (b) Electron trapping in the AlGaN with a density of 10^{17}cm^{-3}, ranging in extent from the AlGaN/GaN interface to a distance 10 nm from the interface, emulating trapping for higher stress time, such as 100s. The trap energy level is shown for each trapping situation with a dashed line ($E_{t,10s}$ and $E_{t,100s}$ respectively). Since a trap with $E_a \sim 0.6$ eV is observed experimentally, we choose this trap to demonstrate the effect of stress time on trap response time. Although the results are discussed for traps in AlGaN, qualitatively the same arguments and conclusions hold for traps in the GaN buffer.

For an electron trapped in a defect level in the AlGaN barrier, there are two possible detrapping mechanisms. Thermal emission to the conduction band (shown by the vertical solid arrow in Fig. 5a is possible, and is the conventional view. However, another parallel avenue is possible. The two-dimensional electron gas (2DEG) penetrates for some distance into the AlGaN, and as Fig. 5b shows, the 2DEG wavefunction decays rapidly in

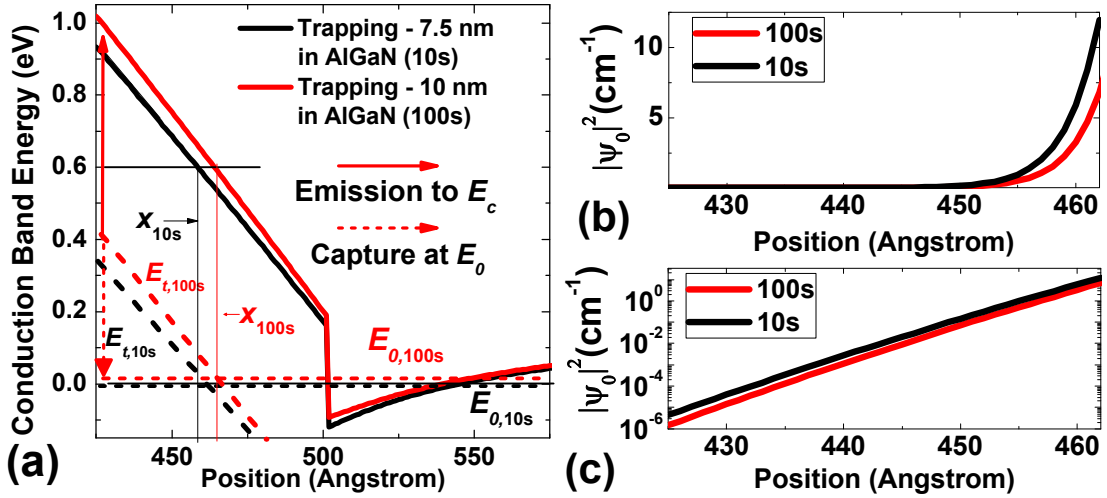

Fig. 5. (a) Simulated conduction band profiles, ground state energy $E_{0,}$ and trap position $E_t \approx E_c - 0.6$ eV for trapping in AlGaN from the heterointerface to a physical depth 7.5 nm and 10 nm away from the interface, emulating short and long duration stresses respectively. Simulated ground-state wavefunction in the AlGaN barrier for the two cases are shown on linear (b) and log (c) scales.

the AlGaN barrier. Thus, at position x, if the wavefunction for the n^{th} 2DEG state with energy E_n is given by $\psi_n(x)$, and the effective density of this state is given by $|\psi_n(x)|^2 D$, where D is the density of states of the two-dimensional band, given by:

$$D = (8\pi m k_B T \ln 2)/h^2 \qquad (2)\ [20]$$

Thus, for a defect at position x close to the heterointerface, once stress is discontinued the carriers trapped in the defect level can be captured directly by the 2DEG states with local density $|\psi_n(x)|^2 D$. This process is shown by the vertical dashed arrow in Fig. 5a. Figs. 5b and 5c show the wavefunction profile for the ground state (with energy E_0) for the two stress times 10s and 100s on linear and log scales.

From Figs. 5b and 5c, we find that the penetration of the wavefunction into the AlGaN barrier decreases as we increase the stress time. This is because as more electrons are trapped in the AlGaN, the conduction band edge rises and increases the barrier height between the GaN and the AlGaN. Thus, the process of capturing electrons trapped in defect states directly by 2DEG states potentially explains both the temperature independence and the stress-time-dependant nature of TG2.

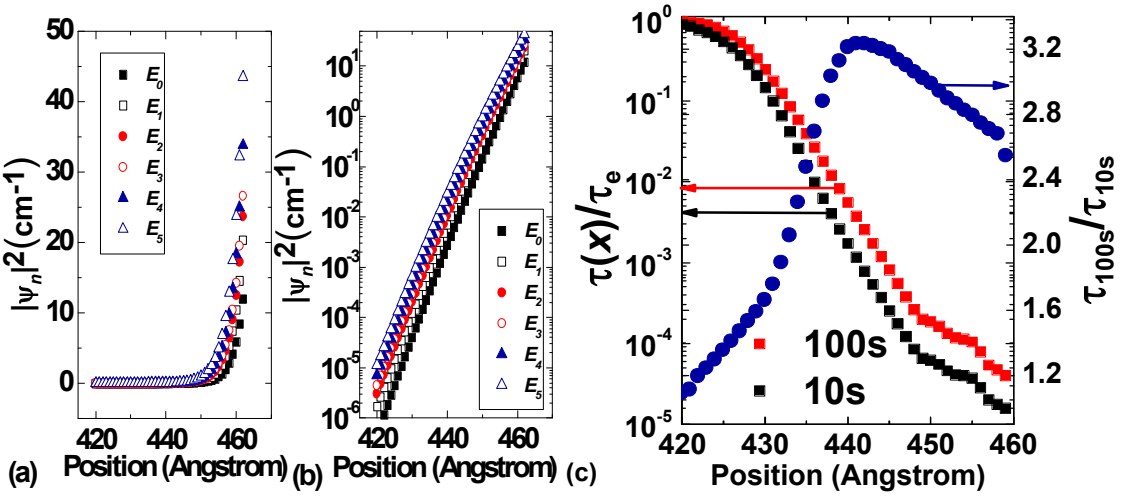

Fig. 6. Decaying tail of the wavefunction into the AlGaN barrier for the six bound states on a a) linear and b) log scales. c) Effective detrapping time constant $\tau(x)$ as a function of position in the AlGaN barrier relative to the bulk emission time constant τ_e for the two trapping magnitudes in Fig. 6, representative of long (100s) and short (10s) stress times. The longer stress time can lead to detrapping time contants that are higher by a factor of ~3.2.

For both the 10s and 100s stress scenarios simulated in Fig. 5, there are six bound states associated with the 2DEG. The higher-energy states show greater penetration into the AlGaN barrier and have a greater effect on the stress-time-dependant behavior (Figs. 6a,b). The capture time constant at an empty defect state in a bulk material is given by $\tau_c = (N_t \sigma v_{th})^{-1}$, where N_t is the density of the level at which capture takes place, σ is the capture cross-section, and v_{th} is the thermal velocity [21]. The captured carriers do not increase the fill fraction of the quantum well states (which are delocalized in the plane of the 2DEG and free to conduct), but rather become part of the drain current. Thus the 2DEG states may be considered to be empty throughout the capture process, and the capture time constant at each of the 2DEG states is given by:

$$\tau_n(x) = (|\psi_n(x)|^2 D\sigma v_{th})^{-1} \quad (3),$$

The thermal emission time constant to the AlGaN band edge is given by $\tau_e = (N_{c,AlGaN}\exp(E_t - E_c)/k_B T)\sigma v_{th})^{-1}$ [21]. At a given position, the sum of all of these processes gives an effective time constant

$$\tau(x) = (\Sigma 1/\tau_n(x) + 1/\tau_e)^{-1} \quad (4)$$

Fig. 6c shows the change in the effective time constant $\tau(x)$ for 10s and 100s stress. E_t is below the Fermi level for the first ~4 nm from the AlGaN/GaN interface, and traps in this region will be filled pre-stress. The Fermi level crossover points for the $E_c - 0.6$ eV trap are denoted as x_{10s} and x_{100s} in Fig. 5a. Direct capture to 2DEG states strongly dominates $\tau(x)$ for the next 3nm, and the response time is less than the thermal emission time constant by several orders of magnitude. Beyond ~7 nm from the heterointerface, $\tau(x)$ is dominated by thermal emission to the conduction band, since the wavefunction rapidly decays into the AlGaN barrier. The enhanced barrier from GaN to AlGaN caused by increased stress time (shown in Fig. 5) causes an overall increase in $\tau(x)$ by a factor that is position dependent and peaks at a value of ~3.2 (Fig. 6c). It is important to note that the increase in time constants between long and short time stresses is most pronounced in a region where $\tau(x)$ shows continuous variation over several orders of magnitude. Figs. 3 and 4 show that the stress-dependant component TG2 spans a much wider range of time constants compared to the thermally activated TG1. This provides another point of consistency between the observed results and the proposed detrapping model.

One might consider the possibility of tunneling from the trap level to the AlGaN barrier conduction band to explain the stress time dependence of TG2. However, this explanation is not consistent with the experimental data. The wavefunction of conduction band states is independent of electric field. As Fig. 5a shows, the increased electron trapping *increases* the electric field for the electron in the barrier-tochannel direction. This reduces the tunneling distance from the trap to the AlGaN conduction band, making the tunneling rate *increase* with stress time (similar to an increase in the tunneling rate from an oxide trap to the semiconductor with increased electric field from oxide to channel in an MOS structure). Therefore, trap to band-edge tunneling also has to be ruled out as a possible explanation for the stress-time dependence of TG2.

The long- and short-time stresses have been emulated in this study by considering two regions of trapping with different thicknesses in the AlGaN barrier. Another alternative to this is to consider trapping over the same spatial location, but with different concentrations. This is plausible, since either increasing the density of trapped charge or the spatial extent of trapping results in an enhanced barrier to electrons from the channel to AlGaN. While quantitative differences will result from different charge distributions in the barrier, increased barrier height due to charging of the barrier reduces the penetration of the wavefunction into the AlGaN, reducing capture into the 2DEG and increasing the overall time constant. For very small penetration, the overall time constant will be close to the bulk emission time constant. Thus, the qualitative nature of the evolution in detrapping time constants with increased stress and current collapse stays the same, independent of variations in trapping location or density.

Design-Dependent Trap Response Time

The variations in the band profile (shown in Fig. 5a) in the direction normal to the 2DEG can be created by design and processing steps such as varying the AlGaN thickness, molefraction, or surface passivation. Thus, the spatial distribution of detrapping time constants (as shown in Fig. 6b), which is an important factor in the switching performance of the HEMT, becomes a function of the process and design parameters controlling the potential barrier profile normal to the 2DEG. For example, a higher AlGaN surface charge density results in a larger electric field in the AlGaN barrier, reducing the coupling between the trap levels and the 2DEG and hence reducing the response time of the traps. Conversely, a higher 2DEG density results in reduced net charge at the heterointerface, since the polarization charge is positive. Therefore, systems with higher 2DEG densities can be expected to have higher coupling between barrier traps and 2DEG levels, reducing the trap response times, all other factors remaining constant. Our results suggest that by using appropriate barrier design techniques, it should be possible to tune the time constant of the recovery of the device following stress, which may be optimized for performance or reliability.

Conclusions

We have demonstrated strong stress-time-dependant behavior of detrapping time constants for near-heterointerface defects in AlGaN/GaN HEMTs under both blocking voltage stress and ON-state conditions. The stress-time-dependant behavior is shown to be consistent with the capture of trapped carriers in the AlGaN barrier directly by quantum well states. The proximity of the quantum well and the penetration of the bound-state wavefunctions into the barrier are shown to reduce the response time of a barrier trap 0.6 eV below the conduction band edge by several orders of magnitude compared to its bulk response time. The electric field normal to the 2DEG is shown to have a strong effect on the trap response time.

Acknowledgments

This work was supported by the GaN Initiative for Grid Applications (GIGA) program managed by Dr. G. Bindewald of the U.S. Department of Energy's Office of Electricity Sandia National Laboratories is a multi-program laboratory managed and operated by Sandia Corporation, a wholly-owned subsidiary of Lockheed Martin Corporation, for the U.S. Department of Energy's National Nuclear Security Administration under contract DE-AC0494AL85000.

References

1. B. Lu and T. Palacios, *IEEE Electron Device Letters*, **31**(9), 951 (2010).
2. N. Tipirneni, A. Koudymov, V. Adivarahan, J. Yang, G. Simin, and M. Asif Khan, **27**(9), 716 (2006).
3. J. Das, J. Everts, J.Van Den Keybus, M. Van Hove, D. Visalli, P. Srivastava, D. Marcon, Kai Cheng, M. Leys, S. Decoutere, J. Driesen, G. Borghs, *Electron Device Letters, IEEE* , **32**(10), 1370 (2011).
4. Y.-F. Wu, M. J. Mitos, M. L. Moore, and S. Heikman, *IEEE Electron Device Lett.*, **29**(8), 824 (2008).

5. D. Pavlidis, P. Valizadeh, and S. H. Hsu, in *Proc. GaAs Symp*., 265 (2005).
6. R. Vetury, N. Q. Zhang, S. Keller, and U. K. Mishra, *IEEE Trans. Electron Devices*, **48**(3), 560 (2001).
7. J. W. Chung, J. C. Roberts, E. L. Piner, and T. Palacios, *IEEE Electron Device Lett.*, **29**(11), 1196 (2008).
8. Jungwoo Joh and J.A. del Alamo, *IEEE Trans. Electron Devices*, **58**(1), 132 (2011).
9. A. Sozza, C. Dua, E. Morvan, M. A. diForte-Poisson, S. Delage, F. Rampazzo, A. Tazzoli, F. Danesin, G. Meneghesso, E. Zanoni, A. Curutchet, N. Malbert, N. Labat, B. Grimbert, and J.-C. De Jaeger, in *IEDM Tech. Dig.*, 590 (2005).
10. T. Mizutani, T. Okino, K. Kawada, Y. Ohno, S. Kishimoto, and K. Mzezawa, *Phys. Stat. Sol. (A)*, **200**(1), 195 (2003).
11. A. Chini, F. Fantini, V. Di Lecce, M. Esposto, A. Stocco, N. Ronchi, F. Zanon, G. Meneghesso, and E. Zanoni, in *IEDM Tech. Dig.*, 1 (2009).
12. M. Tapajna, R. J. T. Simms, Y. Pei, U. K. Mishra, and M. Kuball, *IEEE Electron Device Lett.*, **31**(7), 662 (2010).
13. M. Meneghini, C. de Santi, T. Ueda, T. Tanaka, D. Ueda, E. Zanoni, and G. Meneghesso, *IEEE Electron Device Letters*, **33**(3), 375 (2012).
14. J. Joh and J. A. del Alamo, in *IEDM Tech. Dig.*, 461 (2008).
15. G. Meneghesso, G. Verzellesi, F. Danesin, F. Rampazzo, F. Zanon, A. Tazzoli, M. Meneghini, and E. Zanoni, *IEEE Transacions on Device and Materials Reliability* , **8**(2), 332 (2008).
16. J. A. del Alamo and J. Joh, *Microelectronics Reliability* , **49**(5), 1200 (2009).
17. J. Joh, U. Chowdhury, T. M. Chou, H. Q. Tserng, and J. L. Jimenez, "Method for estimation of the channel temperature of GaN high electron mobility transistors," in *Proc. ROCS Workshop* , 87 (2007).
18. A. Sarua, H. Ji, M. Kuball, M. J. Uren, T. Martin, K. P. Hilton, and R. S. Balmer, *IEEE Trans. Electron Devices* , **53**(10), 2438, (2006).
19. J. Kuzmik, P. Javorka, A. Alam, M. Marso, M. Heuken, and P. Kordos, *IEEE Trans. Electron Devices*, **49**(8), 1496, (2002).
20. John H. Davies, *The Physics of Low Dimensional Semiconductors,* 6th ed. NY: Cambridge University Press, 2006.
21. D. K. Schroder, *Semiconductor Material and Device Characterization*, 3rd ed. Hoboken, NJ: Wiley, 2006.